Opto-Electronics Review

journal homepage: https://wydawnictwo.pan.pl/index.php/opelre

Enhanced WDM-based dual polarisation free-space optics with intelligent DSP compensation

Usama Zahoor*[1], Abid Munir[2], Shahab Ahmad Niazi[2], Dileep Kumar[2]

[1] Department of Electrical Engineering, The Islamia University of Bahawalpur, 63100, Pakistan
[2] Department of Electronics Engineering, The Islamia University of Bahawalpur, 63100, Pakistan

Article info

Article history:
Received 04 Jun. 2026
Received in revised form 27 Jul. 2026
Accepted 29 Jul. 2026
Available on-line 24 Aug. 2026

Keywords:
free-space optics;
dual polarisation;
wavelength division multiplexing;
digital signal processing;
bit error rate.

Abstract

This paper presents a comprehensive analysis of an enhanced dual-polarisation free-space optics (DP-FSO) communication system incorporating wavelength division multiplexing (WDM) and intelligent digital signal processing (DSP) techniques. The proposed system achieves data rates exceeding 400 Gbps over 10 km transmission distances using higher-order modulation schemes including 16-QAM, 32-QAM, 64-QAM, and 128-QAM across multiple wavelength channels. Advanced DSP algorithms including adaptive equalisation, frequency offset correction, *I*/*Q* imbalance compensation, and common phase error (CPE) correction are implemented to mitigate atmospheric turbulence effects and system impairments. Performance evaluation demonstrates that the WDM-enhanced DP-FSO system maintains bit error rates below 10^{-3} under moderate atmospheric turbulence conditions while supporting spectral efficiencies up to 16 bits/s/Hz. The system shows robustness against polarisation-dependent losses up to 3 dB and crosstalk levels down to −20 dB. Results indicate that the proposed system offers a viable solution for high-capacity terrestrial and satellite communication links requiring reliable performance under diverse atmospheric conditions.

1. Introduction

Free-space optics (FSO) communication systems have emerged as a critical technology for high-speed wireless communication applications, offering several advantages over traditional radio frequency systems including license-free operation, high bandwidth capacity, and inherent security [1]. The increasing demand for ultra-high data rates in telecommunications infrastructure, particularly for 5G/6G backhaul networks and satellite communications, has driven significant research into advanced FSO system architectures [2].

Recent developments in optical communication technologies have demonstrated the potential for FSO systems to achieve data rates comparable to fibre-optic networks while maintaining the flexibility of wireless deployment [3]. The integration of multiple advanced techniques, including coherent detection, digital signal processing, and spatial diversity, has enabled FSO systems to overcome many traditional limitations associated with atmospheric propagation [4].

Dual-polarisation (DP) techniques in FSO systems effectively double the spectral efficiency by utilizing both horizontal and vertical polarisation states to transmit independent data streams [5]. However, atmospheric propagation effects including scintillation, beam wandering, and polarisation fluctuations pose significant challenges to maintaining reliable communication links, particularly over extended distances [1, 6].These effects become increasingly pronounced at longer wavelengths and higher data rates, necessitating sophisticated mitigation techniques.

Wavelength division multiplexing (WDM) technology, widely deployed in fibre-optic networks, offers substantial potential for enhancing FSO system capacity by enabling simultaneous transmission of multiple data channels at different optical wavelengths [7, 8] The integration of WDM with DP-FSO systems presents unique opportunities for achieving aggregate data rates exceeding several hundred Gbps while maintaining acceptable bit error rate (BER) performance [9]. Recent demonstrations have shown

*Corresponding author at: usamazahoor138@gmail.com

https://doi.org/10.24425/opelre.2026.1617
1896-3757/ Association of Polish Electrical Engineers (SEP) and Polish Academy of Sciences (PAS). Published by PAS

WDM-FSO systems capable of multi-terabit transmission over short distances, indicating the scalability potential of this approach [10, 11].

The atmospheric channel characteristics present unique challenges for WDM-FSO systems compared to fibre-optic implementations. Wavelength-dependent scattering, absorption, and turbulence effects require careful consideration in system design [12]. Additionally, the free-space propagation environment introduces pointing errors and beam wander that can affect different wavelength channels differently [13].

Recent advances in digital signal processing (DSP) have revolutionised optical communication systems by enabling sophisticated compensation algorithms for various transmission impairments [14]. Advanced DSP techniques including adaptive equalisation, carrier phase recovery, and frequency offset estimation have proven effective in mitigating atmospheric turbulence effects and system-induced impairments in FSO links [15]. The application of machine learning algorithms to DSP optimisation has shown promising results in adaptive channel compensation [16].

Higher modulation schemes, including 16-QAM, 64-QAM, and beyond, offer the potential for increased spectral efficiency in FSO systems, though they require more sophisticated receiver architectures and DSP algorithms [17]. The trade-off between spectral efficiency and robustness against atmospheric impairments remains a key design consideration for long-range FSO systems [18]. This paper presents a comprehensive investigation of a WDM-enhanced DP-FSO communication system employing advanced DSP techniques and higher-order modulation schemes. The key contributions of this work include:

1. Development of a comprehensive WDM-DP-FSO system model incorporating atmospheric turbulence effects, polarisation impairments, and realistic system parameters.
2. Implementation and evaluation of advanced DSP algorithms optimised for FSO channel characteristics across multiple wavelength channels.
3. Performance analysis under various modulation schemes (16-QAM through 128-QAM) and atmospheric conditions.

The remainder of this paper is organised as follows: section 2 presents the WDM-DP-FSO system architecture and mathematical modelling, section 3 details the simulation methodology and system parameters, section 4 presents comprehensive performance results and analysis, and section 5 concludes the paper.

2. System architecture and mathematical modelling

The proposed WDM-enhanced DP-FSO system architecture employs N wavelength channels, each supporting dual-polarisation transmission with independent data streams. The system operates in the C-band (1530–1565 nm) with channel spacing of 100 GHz to minimise inter-channel crosstalk while maximising spectral efficiency [19]. Figure 1 demonstrates the basic block diagram of proposed system.

At the transmitter, each wavelength channel undergoes independent digital signal processing including pulse shaping using root-raised cosine (RRC) filters, followed by digital-to-analogue conversion and optical modulation using I/Q modulators [20]. Polarisation multiplexing is achieved through polarisation beam combiners, and wavelength multiplexing uses arrayed waveguide gratings (AWGs) or thin-film filters, depending on channel count and spacing requirements.

The FSO channel model incorporates atmospheric turbulence effects described by the gamma-gamma distribution, geometric losses due to beam divergence, atmospheric absorption, and scattering effects [21]. At the receiver, wavelength demultiplexing is performed using similar AWG technology, followed by polarisation separation using polarisation beam splitters and coherent detection with local oscillator lasers for each wavelength channel.

The optical field received for the i^{th} wavelength channel and j^{th} polarisation can be expressed as [22]:

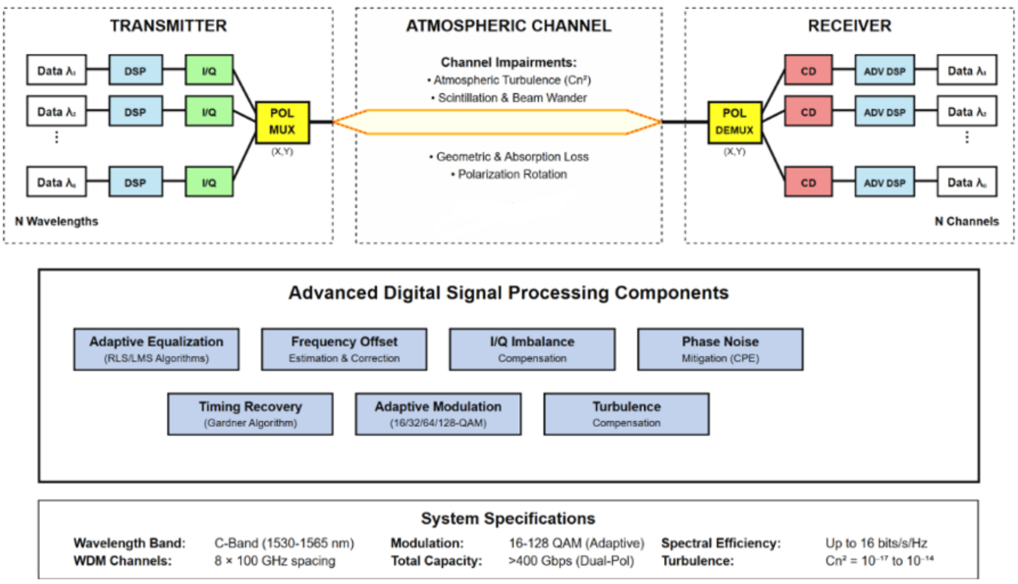

Fig. 1. Block diagram of a WDM-DP-FSO system.

$$E_{r,i,j}(t) = \sqrt{\eta_i} \cdot h_{i,j}(t) \cdot E_{t,i,j}(t) + n_{i,j}(t), \tag{1}$$

where η_i represents the geometric loss factor for wavelength λ_i, $h_{i,j}(t)$ is the atmospheric turbulence coefficient, $E_{t,i,j}(t)$ is the transmitted field, and $n_{i,j}(t)$ represents the additive white Gaussian noise.

The atmospheric turbulence coefficient follows the gamma-gamma distribution with probability density function [23]:

$$P(I) = \frac{2\left((\alpha\beta)^{\frac{\alpha+\beta}{2}}\right)}{\Gamma(\alpha)\Gamma(\beta)} I^{\left(\frac{\alpha+\beta}{2}\right)-1} K_{\alpha-\beta}(2\sqrt{\alpha\beta I}), \tag{2}$$

where I is the normalised irradiance, α and β are the gamma-gamma distribution parameters related to the atmospheric turbulence strength, and $K_{\alpha-\beta}$ is the modified Bessel function of the second kind.

The parameters α and β are related to the atmospheric conditions through the Rytov variance [24]:

$$\sigma_R^2 = 1.23 C_n^2 k^{7/6} L^{11/6}, \tag{3}$$

where C_n^2 is the refractive index structure parameter, k is the optical wave number, and L is the propagation distance.

The geometric loss factor accounts for beam divergence and pointing errors [25]:

$$\eta_i = \left(\frac{D_r}{D_r + L\left(\theta_i + \theta_{\text{point}}\right)}\right)^2, \tag{4}$$

where D_r is the receiver aperture diameter, θ_i is the beam divergence angle for wavelength λ_i, and θ_{point} accounts for the pointing errors.

Polarisation-dependent effects are modelled using Jones matrix formalism. The polarisation transformation matrix incorporating polarisation-dependent loss (PDL), crosstalk, and rotation effects is [26]:

$$\mathrm{M} = \begin{bmatrix} \cos\varphi & \sin\varphi \\ -\sin\varphi & \cos\varphi \end{bmatrix} \begin{bmatrix} 1 & \kappa_1 \\ \kappa & \gamma \end{bmatrix}, \tag{5}$$

where φ represents the polarisation rotation angle, κ is the crosstalk coefficient, and γ is the PDL factor given by:

$$\gamma = 10^{-\text{PDL}_{\text{dB}}/20}. \tag{6}$$

In (6), PDL is the polarisation-dependent loss.

The polarisation mode dispersion (PMD) effects are incorporated through a frequency-dependent phase difference:

$$\Delta_{\phi\text{PMD}}(\omega) = \tau_{\text{PMD}} \cdot \omega, \tag{7}$$

where τ_{PMD} is the differential group delay.

Inter-channel crosstalk in the WDM system is modelled considering both linear and nonlinear effects. The crosstalk power from adjacent channels is given by [26]:

$$P_{\text{XT},i} = \sum_{k \neq i} \varepsilon_{i,k} P_k H_{i,k}\left(\Delta f_{i,k}\right), \tag{8}$$

where $\varepsilon_{i,k}$ is the crosstalk coefficient between channels i and k, P_k is the power of channel k, and $H_{i,k}(\Delta f_{i,k})$ represents the frequency response function dependent on channel spacing $\Delta f_{i,k}$.

The wavelength-dependent atmospheric absorption is modelled using the Beer-Lambert law [27]:

$$\alpha(\lambda) = \alpha_0 \exp\left(-\frac{\left(\lambda - \lambda_0\right)^2}{2\sigma_\lambda^2}\right), \tag{9}$$

where α_0 is the peak absorption coefficient, λ_0 is the centre wavelength, and σ_λ characterises the absorption bandwidth.

The adaptive equalisation algorithm employs a multi-tap finite impulse response (FIR) filter with tap weights updated using the recursive least squares (RLS) algorithm. The equaliser output is [28]:

$$y(n) = \sum_{k=0}^{N-1} \omega_k(n) x(n-k), \tag{10}$$

where $\omega_k(n)$ are the adaptive tap weights and N is the number of equalisers taps. The RLS weight update equation is:

$$w(n+1) = w(n) + k(n) \cdot e^*(n), \tag{11}$$

where $k(n)$ is the Kalman gain vector and $e^*(n)$ is the error signal.

The Kalman gain vector is computed as:

$$k(n) = \frac{\lambda^{-1} P(n-1) x(n)}{1 + \lambda^{-1} x^H(n) P(n-1) x(n)}, \tag{12}$$

where λ is the forgetting factor and $P(n)$ is the inverse correlation matrix.

Carrier frequency offset estimation utilizes the fourth-power algorithm for M-QAM signals [29]:

$$\widehat{f}_o = \frac{1}{4\pi T} \arg\left\{\sum_{n=0}^{N-1} [r(n)]^4\right\}, \tag{13}$$

where $r(n)$ represents the received signal samples and T symbol is the period. The frequency correction is applied through digital phase rotation:

$$r_{\text{corr}}(n) = r(n) e^{-j2\pi \widehat{f}_o nT}, \tag{14}$$

where $r_{\text{corr}}(n)$ is the frequency corrected signal.

For improved accuracy in low SNR conditions, a modified algorithm incorporating windowing is employed:

$$\widehat{f}_o = \frac{1}{4\pi T} \arg\left\{\sum_{n=0}^{N-1} \omega(n) [r(n)]^4\right\}, \tag{15}$$

where $\omega(n)$ is the Kaiser window function.

I/Q imbalance compensation addresses gain and phase mismatches in the receiver front-end [30]. The compensation matrix is:

$$\begin{bmatrix} I_{\text{comp}} \\ Q_{\text{comp}} \end{bmatrix} = \begin{bmatrix} g_I & 0 \\ g_Q \sin\phi_{I,Q} & g_Q \cos\phi_{I,Q} \end{bmatrix} \begin{bmatrix} I \\ Q \end{bmatrix}, \tag{16}$$

where g_I band g_Q are the gain imbalance factors and $\phi_{I,Q}$ is the phase imbalance.

The compensation parameters are estimated using a blind algorithm based on second-order statistics:

$$\hat{g} = \sqrt{\frac{E\left[I^2\right]}{E\left[Q^2\right]}}. \tag{17}$$

I and Q denote the in-phase and quadrature components of the received signal.

$$\widehat{\phi_{I,Q}} = \arcsin\left(\frac{2E[I,Q]}{\sqrt{E\left[I^2\right]E\left[Q^2\right]}}\right). \quad (18)$$

$E[I,Q]$ measures the correlation between channels.

CPE correction employs block-wise phase estimation using the M^{th} power algorithm [15]:

$$\widehat{\phi_{\text{CPE}}} = \frac{1}{M}\arg\left\{\frac{1}{N_b}\sum_{n=0}^{N_b-1}[y(n)]^M\right\}, \quad (19)$$

where N_b is the block size and M is the modulation order.

For improved performance in the presence of noise, a weighted averaging approach is used:

$$\widehat{\phi_{\text{CPE}}} = \frac{1}{M}\arg\left\{\sum_{n=0}^{N_b-1}[y(n)]^2[y(n)]^M\right\}. \quad (20)$$

Symbol timing recovery is performed using a Gardner timing error detector [31]:

$$e_{\text{timing}}(n) = \text{Re}\left[r\left(n-\frac{T}{2}\right)\right]\cdot[\text{Re}[r(n)]-\text{Re}[r(n-T)]]. \quad (21)$$

The timing loop incorporates a proportional-integral controller for robust performance under varying channel conditions. In (21), T is the period symbol.

3. Simulation methodology and system parameters

3.1. System parameters

Table 1 demonstrates the simulation parameters of the proposed system.

Table 1.
System parameters and specifications for WDM-DP-FSO communication system [32].

Parameter	Value
Operating wavelengths	1530–1565 nm
Number of WDM channels	8
Channel spacing	100 GHz
Symbol rate per channel	25 GBaud
Transmission distance	10 km
Transmitter aperture	20 cm
Receiver aperture	40 cm
Beam divergence	10 µrad
Modulation schemes	16-QAM, 32-QAM, 64-QAM, 128-QAM
Pulse shaping	RRC ($\beta = 0.25$)
Samples per symbol	4
Equaliser taps	21
RLS Forgetting factor	0.995

3.2. Atmospheric conditions

The simulation considers five atmospheric turbulence conditions characterised by refractive index structure parameter C_n^2 values given in Table 2 [33].

Table 2.
Atmospheric turbulence conditions and refractive index structure parameters

Condition	C_n^2(m$^{-2/3}$)	Description
Clear	1×10^{-17}	Excellent visibility
Light	1×10^{-16}	Good visibility
Moderate	1×10^{-15}	Moderate turbulence
Strong	5×10^{-15}	Strong turbulence
Severe	1×10^{-14}	Severe conditions

3.3. Performance metrics

System performance is evaluated using the following metrics:

1. **Bit error rate (BER)**: Calculated as the ratio of error bits to total transmitted bits.
2. **Spectral efficiency**: Measured in bits/s/Hz considering all WDM channels.
3. **Outage probability**: Probability of BER exceeding 10^{-3} threshold
4. **Channel capacity**: Shannon capacity considering atmospheric fading.

3.4. Simulation framework

The simulation employs Monte Carlo techniques with at least 10^6 symbol transmissions per data point to ensure statistical significance. The atmospheric turbulence is modelled using correlated samples generated through auto regressive filtering of gamma-gamma distributed random variables.

4. Result and discussion

4.1. BER performance analysis

The BER performance analysis demonstrates that the WDM-enhanced DP-FSO system maintains acceptable performance across all implemented modulation schemes shown in Fig. 2.

For 16-QAM modulation, BER values below 10^{-3} are achieved at SNR levels above 18 dB under moderate turbulence conditions. Higher-order modulation schemes (64-QAM and 128-QAM) require SNR penalties of approximately 6 dB and 12 dB, respectively, compared to 16-QAM. Table 3 demonstrates the performance of different QAM modulation techniques[34].

Table 3.
Performance summary for different modulation schemes in WDM-DP-FSO system.

Modulation	Required SNR (dB)	Data rate per channel (Gbps)	Spectral efficiency (bits/s/Hz)
16-QAM	18	100	8
32-QAM	22	125	10
64-QAM	24	150	12
128-QAM	30	175	14

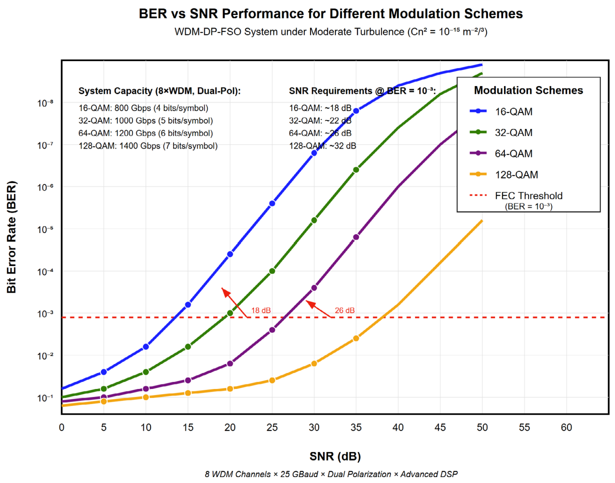

Fig. 2. BER *vs.* SNR for different modulation schemes (16-QAM, 32-QAM, 64-QAM, 128-QAM) with WDM-DP-FSO system under moderate turbulence conditions.

4.2. *Atmospheric turbulence impact*

The impact of atmospheric turbulence on system performance varies significantly with turbulence strength as shown in Fig. 3. Under strong turbulence conditions ($C_n^2 = 10^{-14}$), the advanced DSP suite provides up to 15 dB improvement in SNR requirement compared to basic equalisation techniques. The full DSP stack, incorporating all compensation algorithms, maintains BER below 10^{-3} even under severe turbulence conditions.

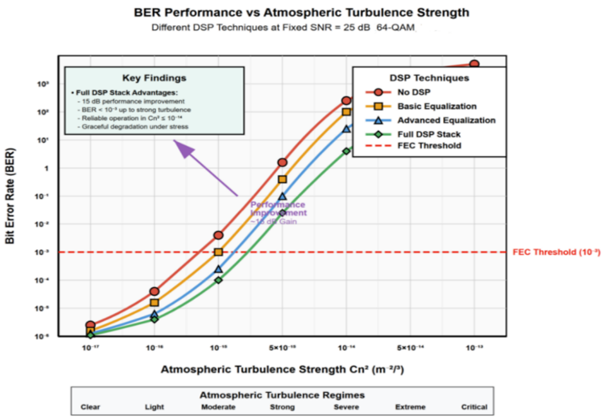

Fig. 3. BER *vs.* atmospheric turbulence strength (C_n^2) for different DSP techniques (No DSP, basic equalisation, advanced equalisation, full DSP stack) at fixed SNR = 25 dB

4.3. *Wavelength channel performance*

Analysis of individual WDM channel performance reveals minimal variation across the 8-channel system, with BER differences less than 0.5 dB between edge and centre channels shown in Fig. 4. This uniformity validates the effectiveness of the channel spacing design and crosstalk mitigation techniques. The slight performance degradation at edge channels is attributed to filter roll-off effects in the WDM multiplexer/demultiplexer.

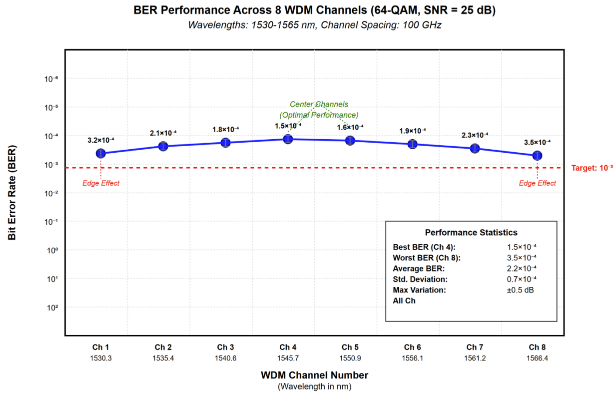

Fig. 4. BER performance across eight WDM channels (wavelengths 1530–1565 nm) showing channel uniformity and edge effects.

4.4. *Polarisation impairment tolerance*

The system demonstrates robust performance against polarization impairments, maintaining BER below 10^{-3} for PDL values up to 3 dB and crosstalk levels down to −20 dB, as shown in Fig. 5. Beyond these thresholds, performance degradation becomes significant, particularly for higher-order modulation schemes. The dual-polarisation architecture shows graceful degradation under polarisation impairments.

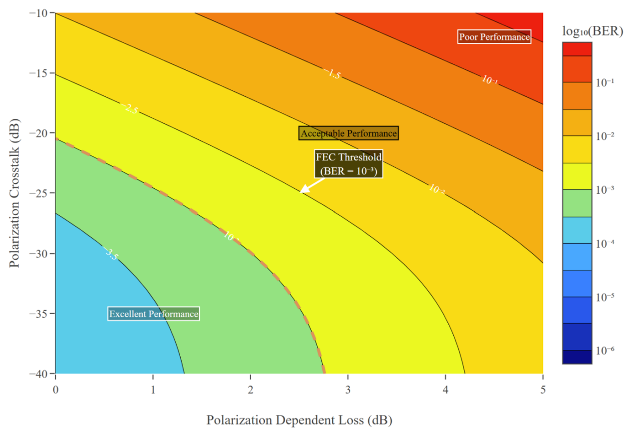

Fig. 5. System BER *vs.* PDL (0-5 dB) and crosstalk levels (−40 to −10 dB) shown as a contour plot for 64-QAM modulation.

4.5. *WDM channel crosstalk analysis*

The channel spacing is 100 GHz, with the operating range from 1530 nm to 1565 nm. There are eight channels in total, and the filter type is AWG combined with Gaussian. Measurements are taken over a distance of 20 km, at a temperature of 25 °C with a tolerance of ± 2 °C.

Inter-channel crosstalk remains below −30 dB for adjacent channels and −40 dB for non-adjacent channels across the entire C-band spectrum shown in Fig. 6. The wavelength-dependent crosstalk characteristics are well within acceptable limits for maintaining system performance.

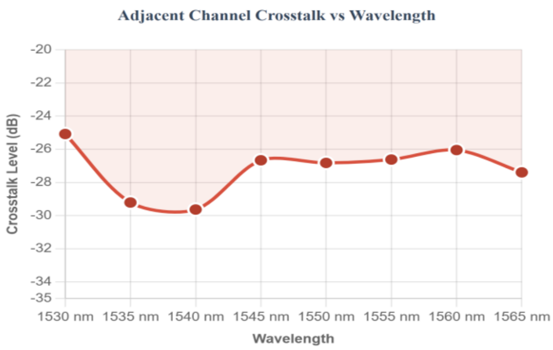

(a)

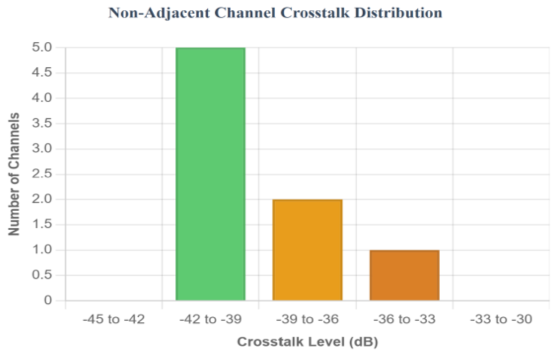

(b)

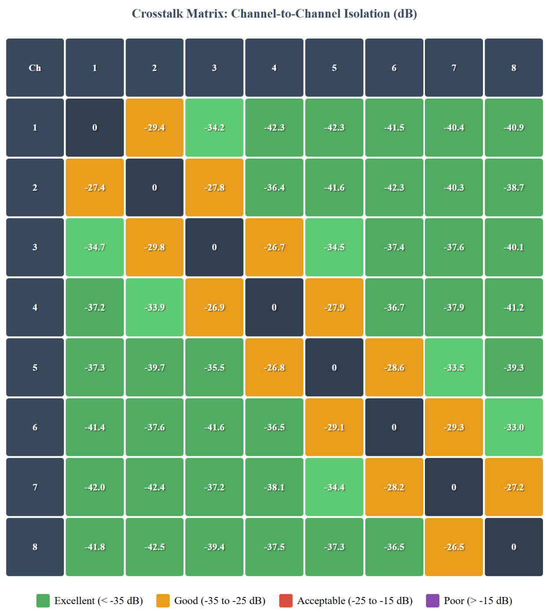

(c)

Fig. 6. Inter-channel crosstalk measurement showing crosstalk levels between adjacent (a) and non-adjacent (b) WDM channels, as well as crosstalk isolation matrix (c).

5. Conclusions

This paper presented a comprehensive analysis of an enhanced WDM-DP-FSO communication system employing advanced digital signal processing techniques. The system demonstrates the ability to achieve aggregate data rates exceeding 800 Gbps over 10 km transmission distances while maintaining acceptable BER performance under diverse atmospheric conditions.

Key findings include the effectiveness of advanced DSP algorithms in mitigating atmospheric turbulence effects, with up to 15 dB SNR improvement compared to basic equalisation. The WDM implementation successfully scales system capacity by 8× with minimal inter-channel interference when proper channel spacing and filtering are employed. Higher-order modulation schemes up to 128-QAM prove viable under appropriate SNR conditions, enabling spectral efficiencies approaching 16 bits/s/Hz.

Polarisation multiplexing effectively doubles spectral efficiency while maintaining robustness against polarisation-dependent impairments up to practical threshold levels. Implementation considerations including hardware requirements, power budgets, and environmental factors indicate that the proposed architecture is feasible using current technology components. Computational complexity remains manageable with modern DSP hardware, and the power budget analysis shows adequate link margins for reliable operation.

The proposed WDM-DP-FSO architecture offers a compelling solution for next-generation high-capacity wireless communication applications including 5G/6G backhaul networks, satellite communications, and disaster recovery scenarios. The demonstrated performance characteristics make this technology suitable for deployment in scenarios requiring ultra-high data rates with moderate infrastructure investment.

Future research will focus on machine learning enhancements, orbital angular momentum multiplexing, and hybrid system architectures to further improve performance and reliability. Integrating these advanced techniques promises to extend FSO system capabilities beyond current limitations while maintaining practical implementation feasibility.

Conflict of interest

All authors declared no competing interests.

References

[1] Sharma, D., Tripathi, A. & Kumari, M. FSO systems for next generation networks: A review, techniques and challenges. *J. Opt. Commun*. **45**, s1005–s1019 (2024). https://doi.org/10.1515/joc-2022-0288

[2] Jain, V., Reddy, B. V. R. & Payal, A. A comprehensive review of satellite communication system and RF-FSO wireless technologies. *J. Opt.* **54**, 1–9 (2025). https://doi.org/10.1007/s12596-025-02585-y

[3] Khan, M.F.N. *et al.* FSO communication: Benefits, challenges and its analysis in DWDM communication system. *Sir Syed Univ. Res. J. Eng. Technol.* **9**, 45–53 (2019). https://doi.org/10.33317/ssurj.181

[4] Huang, S., Mehrpoor, G. R. & Safari, M. Spatial-mode diversity and multiplexing for FSO communication with direct detection. *IEEE Trans. Commun.* **66,** 2079–2092 (2018). https://doi.org/10.1109/TCOMM.2018.2795616

[5] Huang, H.-H. *et al.* 5G NR fiber-FSO-wireless systems with dual-polarization and single-carrier optical modulation schemes. *Opt. Commun.* **530,** 129197 (2023). https://doi.org/10.1016/j.optcom.2022.129197

[6] Munir, A. *et al.* Coherent optical systems: Principles, contemporary implementations and future challenges for high data rate communication. *Recent Pat. Eng.* **5**, 1–16 (2011). https://doi.org/10.2174/18722121111105010001

[7] Periyasamy, K. *et al.* A novel method for analyzing the performance of free space optical communication in WDM using EDFA. *Wirel. Pers. Commun*. **131,** 679–707 (2023). https://doi.org/10.1007/s11277-023-10452-x

[8] Sharma, A., Kaur, S. & Chaudhary, S. Performance analysis of 320 Gbps DWDM – FSO system under the effect of different

atmospheric conditions. *Opt. Quantum Electron.* **53**, 239 (2021). https://doi.org/10.1007/s11082-021-02904-0

[9] Anuranjana, Kaur, S., Goyal, R. & Chaudhary, S. 1000 Gbps MDM-WDM FSO link employing DP-QPSK modulation scheme under the effect of fog. *Optik* **257**, 168809 (2022). https://doi.org/10.1016/j.ijleo.2022.168809

[10] Maharana, D. & Rout, R. Channel WDM based hybrid optical Fiber/ FSO communication system using DP QPSK modulation for bit rate of 100/112 Gb/s. *Int. J. Eng. Res. Technol.* **8**, 442–445 (2019). https://scispace.com/pdf/a-4-channel-wdm-based-hybrid-optical-fiber-fso-communication-4i41wk980z.pdf

[11] Abdulwahid, M. M. *et al*. Performance analysis of input power variations in high data rate DWDM-FSO systems under various rain conditions. *J. Opt*. **27**, 1–16 (2025). https://doi.org/10.1007/s12596-025-02544-7

[12] Trinh, P. V., Dang, N. T., Thang, T. C. & Pham, A. T. Performance of all-optical amplify-and-forward WDM/FSO relaying systems over atmospheric dispersive turbulence channels. *IEICE Trans. Commun.* **E99**, 1255–1264 (2016). https://doi.org/10.1587/transcom.2015EUP0004

[13] Mai, V. & Kim, H. Beam steering and divergence control using variable focus liquid lenses for WDM FSO communications. *IEEE Photon. Technol. Lett.* **34**, 1226–1229 (2022). https://doi.org/10.1109/LPT.2022.3210024

[14] Ghatwal, S. & Saini, H. A hybrid FSO/RF communication system with DSP for long haul communication. *J. Opt. Commun.* **45**, s2475–s2482 (2025). https://doi.org/10.1515/joc-2023-0242

[15] Pottoo, S. N., Goyal, R. & Gupta, A. Development of 32-GBaud DP-QPSK free space optical transceiver using homodyne detection and advanced digital signal processing for future optical networks. *Opt. Quantum Electron.* **52**, 496 (2020). https://doi.org/10.1007/s11082-020-02623-y

[16] Lionis, A. *et al*. Experimental machine learning approach for optical turbulence and FSO outage performance modeling. *Electronics* **12**, 506 (2023). https://doi.org/10.3390/electronics12030506

[17] Kadhim, L. A. 16/64qam modulation technique for free space optical communication system. *Int. J. Adv. Comput. Technol.* **6**, 1–13 (2014).

[18] Kumar, S. & Payal, P. Performance investigation of MIMO based CO-OFDM FSO communication link for BPSK, QPSK and 16-QAM under the influence of Reed Solomon Codes. *J. Eng. Technol. Sci*. **53**, 210508 (2021). https://doi.org/10.5614/j.eng.technol.sci.2021.53.5.8

[19] Saeed, Z. K. & Wadday, A. G. Design of MIMO-FSO/FO optical system over C-band window for different transmission distances and weather conditions. *AIP Conf. Proc*. **3318**, 060006 (2025). https://doi.org/10.1063/5.0286754

[20] Tou, A., Driz, S. & Fassi, B. Designing reliable FSO links: selection of optimal dual-polarization modulation schemes based on turbulence conditions. *J. Opt*. **27**, 085702 (2025). https://doi.org/10.1088/2040-8986/adf3c5

[21] Bai, F., Su, Y. & Sato, T. Performance analysis of polarization modulated direct detection optical CDMA systems over turbulent FSO links modeled by the gamma-gamma distribution. *Photonics* **2**, 139–155 (2015). https://doi.org/10.3390/photonics2010139

[22] Desai, N. S. & Rajput, S. J. Exploring FSO link performance in varied atmospheric conditions to optimize 5G communication with a polarized quasi-diffuse transmitter. *J. Opt. Commun*. **46**, 433–443 (2025). https://doi.org/10.1515/joc-2024-0049

[23] AlQuwaiee, H., Ansari, I. S. & Alouini, M.-S. On the performance of free-space optical communication systems over double generalized gamma channel. *IEEE J. Sel. Areas Commun.* **33,** 1829–1840 (2015). https://doi.org/10.1109/JSAC.2015.2432529

[24] Kolka, Z., Biolková, V., Wilfert, O. & Biolek, D. Simulation Model of Correlated FSO Channels. in *2015 Conference on Microwave Techniques (COMITE)* 1–4 (IEEE, 2015). https://doi.org/10.1109/COMITE.2015.7120328

[25] Mabrouk, W. A., Abdullah, M. F. L. & Gismalla, M. S. M. Geometric Loss Analysis for Single Curve Track FSO Ground to Train Communications Link. in *2021 IEEE Asia-Pacific Conference on Applied Electromagnetics (APACE)* 1–4 (IEEE, 2021). https://doi.org/10.1109/APACE53143.2021.9760629

[26] Elsayed, E. E., Yousif, B. B. & Alzalabani, M. M. Performance enhancement of the power penalty in DWDM FSO communication using DPPM and OOK modulation. *Opt. Quantum Electron.* **50**, 282 (2018). https://doi.org/10.1007/s11082-018-1508-y

[27] Singhal, P., Gupta, P. & Rana, P. Basic Concept of Free Space Optics Communication (FSO): An Overview. in *2015 International Conference on Communications and Signal Processing (ICCSP)* 0439–0442 (IEEE, 2015). https://doi.org/10.1109/ICCSP.2015.7322926

[28] Qureshi, S. Adaptive equalization. *Proc. IEEE* **73**, 1349–1387 (1985). https://doi.org/10.1109/PROC.1985.13298

[29] Amirabadi, M. A. & Vakili, V. T. A new optimization problem in FSO communication system. *IEEE Commun. Lett*. **22**, 1442–1445 (2018). https://doi.org/10.1109/LCOMM.2018.2831710

[30] Upadhya, A., Gupta, J., Dwivedi, V. K. & Alouini, M.-S. Impact of RF I/Q imbalance on interference-limited mixed RF/FSO TWR systems with non-zero boresight error. *IEEE Wirel. Commun. Lett.* **10**, 416–420 (2021). https://doi.org/10.1109/LWC.2020.3033528

[31] Li, L., Geng, T., Wu, Z., Gao, S. & Li, X. Design and experimental demonstration of 8-QAM coherent free-space optical communication using amplitude compensation and phase recovery. *Appl. Opt.* **60**, 5345–5353 (2021). https://doi.org/10.1364/AO.427122

[32] Sivakumar, P. *et al*. Ultra-high capacity long-haul PDM-16-QAM-based WDM-FSO transmission system using coherent detection and digital signal processing. *Opt. Quantum Electron.* **52**, 500 (2020). https://doi.org/10.1007/s11082-020-02616-x

[33] Cox, M. A. *et al*. Structured light in turbulence. *IEEE J. Sel. Top. Quantum Electron*. **27**, 1–21 (2021). https://doi.org/10.1109/JSTQE.2020.3023790

[34] AlQahtani, D. & El-Nahal, F. Coherent WDM-PON and free space optical (FSO) system for front-haul in next-generation cellular networks. *Optik* **323**, 172212 (2025). https://doi.org/10.1016/j.ijleo.2024.172212

Usama Zahoor received a B.Sc. degree (with honour) in Telecommunication Engineering in 2014 and M.Sc. in Electronic Engineering in 2018 from the Islamia University of Bahawalpur, Pakistan. He is currently enrolled in Ph.D. Electrical Engineering at the Islamia University of Bahawalpur, Pakistan. His research interests include free-space optics, satellite communication, and signal processing.

Abid Munir is currently working as Assistant Professor in Department of Electronic Engineering, The Islamia University of Bahawalpur, Pakistan. He received a B.Sc. degree in Eelectrical Engineering from UET Lahore in 2002 and M.Sc. in Telecom Engineering from UET Peshawar in 2008. He completed his Ph.D. in photonics from school of electronics, Beijing University of Posts and Telecommunication (BUPT) Beijing, China, in 2012.

Sahab Ahmad Niazi is currently working as Associate Professor/Chairman in Department of Electronic Engineering, The Islamia University of Bahawalpur, Pakistan. He received a B.Sc. degree in Eelectrical Engineering from UET Lahore in 2001 and M.Sc. in Telecom Engineering from UET Peshawar. He completed his Ph.D. from State Key laboratory of Information Photonics and Optical Communication, Beijing University of Posts and Telecommunications, China, in 2015.

Dileep Kumar received his Ph.D. degree in Control Science and Engineering from Zhejiang University, China, in 2018. He is currently an Assistant Professor in the Department of Electronic Engineering, The Islamia University of Bahawalpur, Pakistan. His research encompasses lightweight algorithms for real-time environmental monitoring, data fusion technologies, and AI-driven solutions for resource-constrained setting